An Analytical Electric Model for Coupled Inductors with Two Windings in Two-Level Converters

Author(s):
Beck, Simon; Biela, Jürgen

Publication date:
2025

Permanent link:
https://doi.org/https://doi.org/10.3929/ethz-c-000789247

Originally published in:
https://doi.org/10.1109/ecce-europe62795.2025.11238363

An Analytical Electric Model for Coupled Inductors With Two Windings in Two-Level Converters

1st Simon Beck
High Power Electronic Systems (HPE)
D-ITET, ETH Zürich, Switzerland
beck@hpe.ee.ethz.ch

2nd Jürgen Biela
High Power Electronic Systems (HPE)
D-ITET, ETH Zürich, Switzerland
jbiela@ethz.ch

***Abstract*—For many applications, e.g. battery or fuel cell electric vehicles, power electronic converters must achieve a high power density and conduct large DC currents. Hence, many converters require inductors, that can carry a relatively large DC bias current in addition to the ripple current without undergoing saturation. Coupled inductors have been identified as a viable option to achieve a high power density thanks to the (partial) cancellation of the DC magnetic flux in the core material.**

To facilitate a fast converter design, this paper presents an electric model of analytical expressions for the currents (time-domain, DC, RMS), that result in a generalised converter topology that applies rectangular (two-level) voltages with steady-state duty cycles and an arbitrary phase-shift to a two-winding coupled inductor with arbitrary coupling and turns ratio. The presented model is also applicable to converter topologies with transformers, e.g. Dual Active Bridge converters, by setting the DC values of the inductor currents to zero.

***Index Terms*—Coupled inductor, transformer, analytical model, electric model, DC-DC converter, boost converter**

I. Introduction

Numerous power electronics converters with coupled inductors (CIs) have been presented in literature for various applications, e.g. nonisolated DC-DC converters for battery or fuel cell electric vehicles (BEVs, FCEVs) and rectifiers with power factor correction (PFC) [1]–[7]. For these applications, a high power density is desired and large DC currents must be conducted. Converters with CIs have been shown to achieve an up to two-fold increase in power density compared to converters with independent phases, while comparable efficiencies are realised [8]–[10]. This increase in power density stems from the (partial) cancellation of the DC magnetic flux in the magnetic core material of the inversely coupled inductors.

The coupled-inductor boost converter (CIBC) is an example of a converter with a two-winding CI. Its bidirectional variant with switches ($T_{1,\mathrm{II}}$ and $T_{2,\mathrm{II}}$) instead of diodes towards the secondary side is shown in Fig. 1. The CIBC has been analysed in literature w.r.t. the peak-to-peak current ripples of its primary current i_p and of its CI's terminal currents i_1 and i_2 [1], [7], [8], [10].

Another example of a converter with a two-winding CI is the dual floating output boost converter (DFOBC). It has been analysed w.r.t. the resulting current ripples of its CI's terminal and magnetising currents as well as of its input current [5].

However, for both of these exemplary converters (CIBC and DFOBC), a complete steady-state analysis of the time-domain, DC and RMS currents in the CI as well in the switches and the associated DC capacitors is missing in literature.

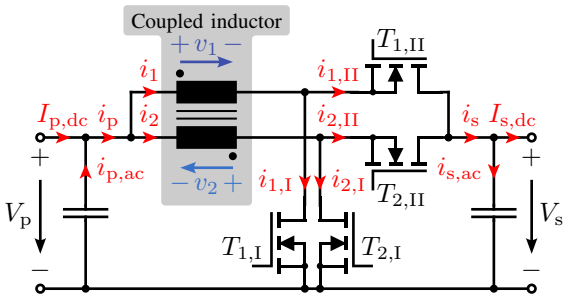

Fig. 1. Bidirectional CIBC with an inversely coupled inductor.

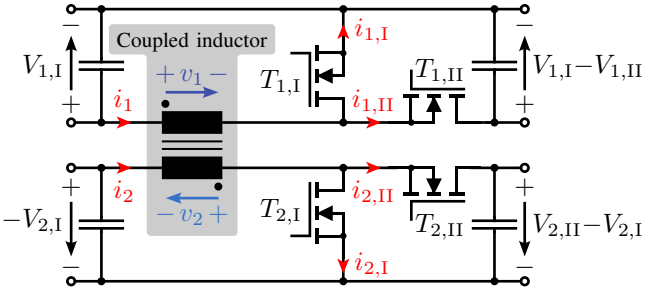

Fig. 2. Generalised two-level topology with an inversely coupled inductor, where $V_{1,\mathrm{I}} > 0\,\mathrm{V}$, $V_{1,\mathrm{II}} < 0\,\mathrm{V}$, $V_{2,\mathrm{I}} < 0\,\mathrm{V}$ and $V_{2,\mathrm{II}} > 0\,\mathrm{V}$ must hold.

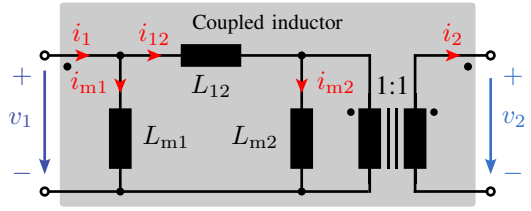

Fig. 3. The equivalent Π circuit of a lossless coupled inductor with an ideal 1:1 transformer, used e.g. in Fig. 1 and Fig. 2.

Therefore, this paper introduces an electric model, which includes explicit analytical expressions for all of these steady-state current values assuming lossless conditions. Furthermore, the model does not only apply to the CIBC or DFOBC topologies because it is based on the generalised converter topology shown in Fig. 2, which applies to many more converters, that generate rectangular (two-level) voltages v_1

and v_2 at the terminals of a CI. Above all, the model even considers possibly unequal duty cycles for the voltages v_1 and v_2, an arbitrary phase shift δ between the voltages, as well as two independent DC bias currents in i_1 and i_2. Lastly, no conditions on the coupling, the turns ratio or the inductance(s) of the CI are imposed. Thanks to the generality of the model, it can also be applied to converter topologies with two-winding transformers, e.g. Dual Active Bridge converters, by setting the DC bias current values to zero.

The paper is structured as follows: The considered equivalent circuit of the CI and the necessary assumptions to apply the presented model are discussed in Section II. The currents in the selected equivalent circuit are analysed in Section III before the resulting analytical expressions for the currents are then stated in Section IV and validated in Section V.

II. Model assumptions

In this section, the necessary assumptions for the electric model of the CI are presented. Namely, the considered equivalent circuit of the two-winding CI, the applied voltage waveforms and the *zero-current startup condition* are introduced.

A. Equivalent circuit of the coupled inductor

The considered CI (or transformer) can have an arbitrary coupling factor and arbitrary (possibly unequal) self-inductances L_1 and L_2. There are multiple equivalent circuits to models such CIs (or transformers) with non-ideal coupling. The T and Π equivalent circuits are popular options. In this paper, the Π circuit, cf. Fig. 3, is chosen to model the CI because its magnetising inductances $L_{\mathrm{m}1}$ and $L_{\mathrm{m}2}$ take the place of the uncoupled self-inductances in the current paths, while the additional inductance L_{12} is associated with the coupling of the inductors in the equivalent circuit. Moreover, the voltages v_1 and v_2 are directly applied to $L_{\mathrm{m}1}$ and $L_{\mathrm{m}2}$ respectively, which leads to simple expressions for the corresponding currents $i_{\mathrm{m}1}$ and $i_{\mathrm{m}2}$. The inductances $L_{\mathrm{m}1}$, $L_{\mathrm{m}2}$ and L_{12} of the Π circuit can be determined with:

$$L_{12}=\tfrac{1-k^2}{k}L_0,\;\; L_{\mathrm{m}1}=\tfrac{1-k^2}{1/n-k}L_0,\;\; L_{\mathrm{m}2}=\tfrac{1-k^2}{n-k}L_0 \quad (1)$$

$$L_0=\sqrt{L_1L_2}=\sqrt{A_{\mathrm{L},1}A_{\mathrm{L},2}}N_1N_2,\;\; n=\sqrt{\tfrac{L_1}{L_2}}=\sqrt{\tfrac{A_{\mathrm{L},1}}{A_{\mathrm{L},2}}}\tfrac{N_1}{N_2} \quad (2)$$

Note that $k\in(0,1)$ in (1) is the coupling factor and n, as defined in (2), is not equal to the turns ratio N_1/N_2 in the general case of unequal permeances $A_{\mathrm{L},1}$ and $A_{\mathrm{L},2}$. It is worth mentioning that, depending on the selected n and/or k, $L_{\mathrm{m}1}$ and $L_{\mathrm{m}2}$ can become negative or even unbounded. In these cases, they do not correspond to physical inductances any more. However, the electric behaviour at the terminals of the CI circuit is still correctly modelled. On the other hand, L_{12} and L_0 are always positive.

With the equivalent circuit defined, the applied voltages v_1 and v_2 are discussed next.

B. Voltages applied to the terminals of the coupled inductor

In this paper, rectangular (two-level) voltages v_1 and v_2 with corresponding duty cycles d_1 and d_2, as defined at the top of Fig. 4, are assumed to be applied to the terminals of the CI (cf. Fig. 3). Both, v_1 and v_2, are periodic in steady state operation with a constant switching period $T_{\mathrm{s}}=1/f_{\mathrm{s}}$. The secondary voltage v_2 may have an arbitrary steady-state phase shift $\delta\in(0,1)$ (normalised to T_{s}) relative to the primary voltage v_1. With the duty cycles and phase shift defined, shorthand notations are introduced at this point:

$$d_1'=1-d_1,\quad d_2'=1-d_2,\quad d_{12}=d_1-d_2,\quad \delta'=1-\delta \quad (3)$$

The switching period is divided into two intervals on each side of the CI, as defined in Fig. 4 for the circuit of Fig. 2:

- *Primary interval I:* $v_1=V_{1,\mathrm{I}}$ ($T_{1,\mathrm{I}}$ conducts)
- *Primary interval II:* $v_1=V_{1,\mathrm{II}}$ ($T_{1,\mathrm{II}}$ conducts)
- *Secondary interval I:* $v_2=V_{2,\mathrm{I}}$ ($T_{2,\mathrm{I}}$ conducts)
- *Secondary interval II:* $v_2=V_{2,\mathrm{II}}$ ($T_{2,\mathrm{II}}$ conducts)

It will become evident in the subsequent analysis that two main cases can be distinguished depending on whether the steady-state switching period starts with *secondary interval II* or *I* as shown in the left and right parts of Fig. 4 respectively:

$$\text{Case A}: d_2+\delta\le 1,\quad \text{Case B}: d_2+\delta>1 \quad (4)$$

With this distinction, the derived electric model will impose no conditions on the signs of $V_{1,\mathrm{I/II}}$ or $V_{2,\mathrm{I/II}}$ as long as steady state can be achieved. However, the circuit that is used to generate v_1 and v_2 might only be capable of generating voltages of a certain polarity. E.g. in the circuit of Fig. 2, $V_{1,\mathrm{I}}>0\,\mathrm{V}$ and $V_{1,\mathrm{II}}<0\,\mathrm{V}$ as well as $V_{2,\mathrm{I}}<0\,\mathrm{V}$ and $V_{2,\mathrm{II}}>0\,\mathrm{V}$ must hold, which is reflected in the waveforms of Fig. 4.

In the CI equivalent circuit given in Fig. 3, steady state is achieved if the time averages (over one switching cycle) of all voltages across the three inductors are zero, which is equivalent to vanishing voltage-time areas at the terminals:

$$\begin{aligned}\textstyle\int_0^{T_{\mathrm{s}}} v_j\mathrm{d}t &= \textstyle\int_{\mathrm{I}} v_j\mathrm{d}t+\int_{\mathrm{II}} v_j\mathrm{d}t,\quad j\in\{1,2\}\\ &= V_{j,\mathrm{I}}d_jT_{\mathrm{s}}+V_{j,\mathrm{II}}d_j'T_{\mathrm{s}}=0\,\mathrm{V\cdot s}\end{aligned} \quad (5)$$

This yields steady-state conditions for the duty cycles in terms of the applied voltages in intervals *I* and *II* as defined in Fig. 4:

$$d_1=\tfrac{V_{1,\mathrm{II}}}{V_{1,\mathrm{II}}-V_{1,\mathrm{I}}}\in(0,1),\quad d_2=\tfrac{V_{2,\mathrm{II}}}{V_{2,\mathrm{II}}-V_{2,\mathrm{I}}}\in(0,1) \quad (6)$$

The steady-state conditions (6) can also be solved for the required steady-state voltages in interval *II* on both sides:

$$V_{1,\mathrm{II}}=-\tfrac{d_1}{d_1'}V_{1,\mathrm{I}},\quad V_{2,\mathrm{II}}=-\tfrac{d_2}{d_2'}V_{2,\mathrm{I}} \quad (7)$$

Since the derived expressions for the resulting currents are found to be simpler if (7) is used, $V_{1,\mathrm{II}}$ and $V_{2,\mathrm{II}}$ are chosen to be eliminated from the subsequent steady-state analysis.

C. CI currents and the zero-current startup condition

Generally, both CI terminal currents i_1 and i_2 (as well as $i_{\mathrm{m}1}$, $i_{\mathrm{m}2}$ and i_{12}) consist of a DC and an AC component:

$$i_j=I_{j,\mathrm{dc}}+i_{j,\mathrm{ac}},\;\; \text{where}\textstyle\int_0^{T_{\mathrm{s}}} i_{j,\mathrm{ac}}\mathrm{d}t=0\,\mathrm{A},\quad j\in\{1,2\} \quad (8)$$

In this paper, the DC components $I_{1,\mathrm{dc}}$ and $I_{2,\mathrm{dc}}$ are assumed to be controlled and therefore known in steady state. Notably, they may be unequal and even have opposite signs.

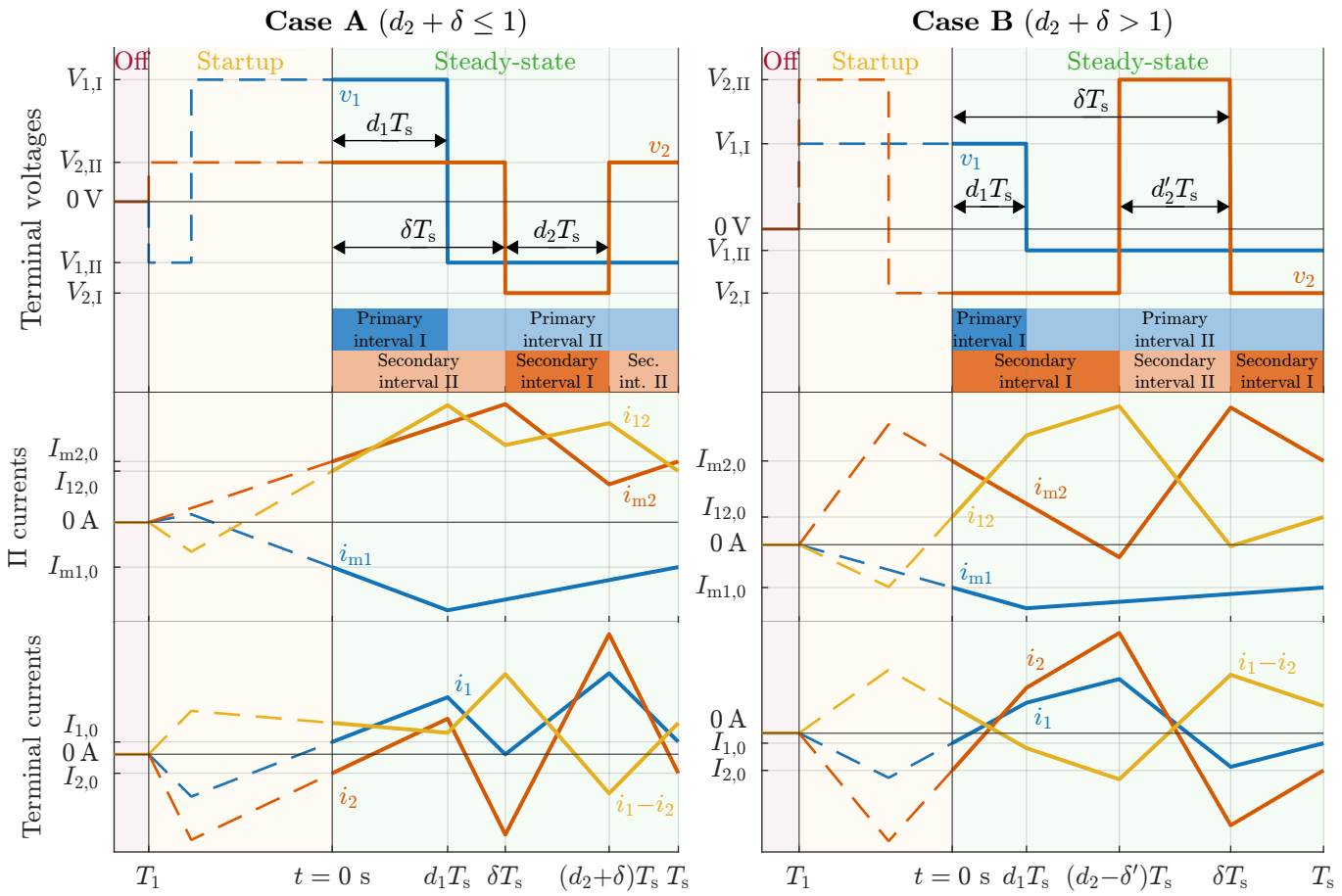

Fig. 4. Exemplary two-level terminal voltages applied to the coupled inductor in Fig. 2 and the resulting currents in the equivalent circuit of Fig. 3. The "Off", and "Startup" intervals are included since all currents are assumed to be zero up to $t=T_1$. Case A ($d_2+\delta\leq 1$) is illustrated on the left-hand side and Case B ($d_2+\delta>1$) on the right-hand side. Intervals I and II are defined for the primary and secondary waveforms in steady-state as indicated. Parameters used for case A: d_1=1/3, d_2=0.3, δ=0.5. Parameters used for case B: d_1=0.2, d_2=0.7, δ=0.75. Common parameters used: $V_{1,\mathrm{I}}$=800 V, $V_{2,\mathrm{I}}$=−600 V, f_s=100 kHz, $I_{1,\mathrm{dc}}$=25 A, $I_{2,\mathrm{dc}}$=10 A, L_0=100 µH, n=2, k=0.9 (i.e. L_{m1}=−47.5 µH, $L_{\mathrm{m2}}\approx$17.273 µH, $L_{12}\approx$21.111 µH).

Finally, all currents are assumed to be initially zero up to a suitable time instant $T_1<0\,\mathrm{s}$, cf. Fig. 4:

$$0\,\mathrm{A}=i_1=i_2=i_{\mathrm{m1}}=i_{\mathrm{m2}}=i_{12}\quad\forall t{\leq}T_1{<}0\,\mathrm{s}\tag{9}$$

This *zero-current startup condition* (9) corresponds to the converter being off prior to T_1 as shown in Fig. 4. During the startup interval $t\in[T_1,0\,\mathrm{s})$, suitable voltages are then assumed to be applied s.t. steady-state operation starts at $t=0\,\mathrm{s}$, which is also illustrated in Fig. 4. This will become important to the analysis of the currents in Section III.

III. Current Analysis

To uniquely identify the steady-state currents in the inductances of the Π circuit of Fig. 3, the currents through all three inductances must be known at least at one point in time because otherwise an arbitrary DC current can be circulating through all three inductances, which would be unaffected by the applied voltages. The *zero-current startup condition* (9) provides such a point in time at $t=T_1$ (and at all points before T_1) when all currents are known to be zero. Therefore, the currents in the magnetising inductances of the Π circuit can be written for $t\geq T_1$ as:

$$i_{\mathrm{m}j}=\underbrace{i_{\mathrm{m}j}(T_1)}_{0\,\mathrm{A}}+\tfrac{1}{L_{\mathrm{m}j}}\textstyle\int_{T_1}^{t}v_j\mathrm{d}t,\quad\forall\,t\geq T_1\quad j\in\{1,2\}\tag{10}$$

The current in L_{12} is now linearly dependent on i_{m1} and i_{m2}:

$$\begin{aligned}i_{12}&=\underbrace{i_{12}(T_1)}_{0\,\mathrm{A}}+\tfrac{1}{L_{12}}\textstyle\int_{T_1}^{t}v_1{-}v_2\mathrm{d}t\quad\forall\,t\geq T_1\\&=\tfrac{1}{L_{12}}\textstyle\int_{T_1}^{t}v_1\mathrm{d}t-\tfrac{1}{L_{12}}\int_{T_1}^{t}v_2\mathrm{d}t\\&=\tfrac{L_{\mathrm{m1}}}{L_{12}}i_{\mathrm{m1}}-\tfrac{L_{\mathrm{m2}}}{L_{12}}i_{\mathrm{m2}}=\tfrac{k}{1/n-k}i_{\mathrm{m1}}-\tfrac{k}{n-k}i_{\mathrm{m2}}\end{aligned}\tag{11}$$

Since (10) and (11) hold at all considered time instants $t\geq T_1$, they can be used to derive the DC components of i_{m1}, i_{m2} and i_{12} next.

A. DC components of i_{m1}, i_{m2} and i_{12}

Thanks to the *zero-current startup condition* (9), and the linear dependence of i_{12} on i_{m1} and i_{m2}, the DC components of i_{m1}, i_{m2} and i_{12} in steady state can be derived as functions

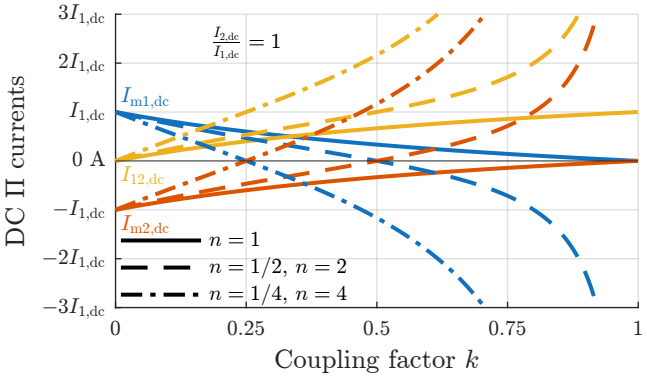

Fig. 5. DC components $I_{\mathrm{m1,dc}}$, $I_{\mathrm{m2,dc}}$ and $I_{12,\mathrm{dc}}$ of i_{m1}, i_{m2} and i_{12} respectively as functions of k and n for $I_{1,\mathrm{dc}} = I_{2,\mathrm{dc}}$.

of the known DC components of the terminal currents. First, the time averages of (10) and (11) are evaluated:

$$I_{\mathrm{m}j,\mathrm{dc}} = \tfrac{1}{T_\mathrm{s}} \int_{0\,\mathrm{s}}^{T_\mathrm{s}} i_{\mathrm{m}j}\mathrm{d}t \quad j \in \{1,2\} \tag{12}$$

$$I_{12,\mathrm{dc}} = \tfrac{1}{T_\mathrm{s}} \int_{0\,\mathrm{s}}^{T_\mathrm{s}} i_{12}\mathrm{d}t = \tfrac{k}{1/n-k} I_{\mathrm{m1,dc}} - \tfrac{k}{n-k} I_{\mathrm{m2,dc}} \tag{13}$$

Second, for the DC components of the terminal currents holds:

$$I_{1,\mathrm{dc}} = I_{\mathrm{m1,dc}} + I_{12,\mathrm{dc}}, \quad I_{2,\mathrm{dc}} = -I_{\mathrm{m2,dc}} + I_{12,\mathrm{dc}} \tag{14}$$

Finally, solving (13) and (14) for $I_{\mathrm{m1,dc}}$, $I_{\mathrm{m2,dc}}$ and $I_{12,\mathrm{dc}}$ results in:

$$I_{\mathrm{m1,dc}} = \tfrac{nI_{1,\mathrm{dc}} - kI_{2,\mathrm{dc}}}{L_{\mathrm{m1}}/L_0}, \quad I_{\mathrm{m2,dc}} = \tfrac{kI_{1,\mathrm{dc}} - I_{2,\mathrm{dc}}/n}{L_{\mathrm{m2}}/L_0} \tag{15}$$

$$I_{12,\mathrm{dc}} = \tfrac{I_{\mathrm{m1,dc}}}{L_{12}/L_{\mathrm{m1}}} - \tfrac{I_{\mathrm{m2,dc}}}{L_{12}/L_{\mathrm{m2}}} = \tfrac{(n-k)I_{1,\mathrm{dc}} + (1/n-k)I_{2,\mathrm{dc}}}{L_{12}/L_0} \tag{16}$$

The main advantage of the inversely coupled inductor is evident in (15) because $I_{\mathrm{m1,dc}}$ and $I_{\mathrm{m2,dc}}$ are calculated based on the (weighted) differences of $I_{1,\mathrm{dc}}$ and $I_{2,\mathrm{dc}}$. This can be understood as if the DC components of the magnetising currents (partially) cancel out depending on the coupling factor k. Fig. 5 illustrates that for $k \to 1$ the DC magnetising currents perfectly cancel out with equal terminal DC currents and $n = 1$. It is evident, that for other choices of n, the perfect cancellation shifts to lower coupling factors (e.g. $k = 1/2$ for $n \in \{1/2, 2\}$ or $k = 1/4$ for $n \in \{1/4, 4\}$) and the DC magnetising currents may even become arbitrarily large for $k \to 1$ and $n \neq I_{2,\mathrm{dc}}/I_{1,\mathrm{dc}}$.

With the DC current components uniquely identified, the initial currents at $t = 0\,\mathrm{s}$ (when steady-state operation is assumed to start) can be derived next.

B. Initial currents at $t = 0\,\mathrm{s}$

With the *zero-current startup condition* (9), applying suitable voltages during the startup interval $t \in [T_1, 0\,\mathrm{s})$ allows for arbitrary initial terminal currents at $t = 0\,\mathrm{s}$ when steady-state operation is started:

$$i_1(0\,\mathrm{s}) = I_{1,0} = \underbrace{\tfrac{1}{L_{\mathrm{m1}}} \int_{T_1}^{0\,\mathrm{s}} v_1 \mathrm{d}t}_{i_{\mathrm{m1}}(0\,\mathrm{s}) = I_{\mathrm{m1},0}} + \underbrace{\tfrac{1}{L_{12}} \int_{T_1}^{0\,\mathrm{s}} v_1 - v_2 \mathrm{d}t}_{i_{12}(0\,\mathrm{s}) = I_{12,0}} \tag{17}$$

$$i_2(0\,\mathrm{s}) = I_{2,0} = -\underbrace{\tfrac{1}{L_{\mathrm{m2}}} \int_{T_1}^{0\,\mathrm{s}} v_2 \mathrm{d}t}_{i_{\mathrm{m2}}(0\,\mathrm{s}) = I_{\mathrm{m2},0}} + \underbrace{\tfrac{1}{L_{12}} \int_{T_1}^{0\,\mathrm{s}} v_1 - v_2 \mathrm{d}t}_{i_{12}(0\,\mathrm{s}) = I_{12,0}} \tag{18}$$

Fig. 4 illustrates possible startup sequences, which use the same voltage levels as are used in steady state. Notably, with fixed CI parameters and predetermined applied voltage levels, there is a limit on how close to $t = 0\,\mathrm{s}$ the time instant T_1 can be chosen.

Because (11) also holds for $t = 0\,\mathrm{s}$, the derivation of $I_{\mathrm{m1},0}$ and $I_{\mathrm{m1},0}$ suffices to fully determine all initial currents. Imposing the previously derived DC components $I_{\mathrm{m1,dc}}$ and $I_{\mathrm{m2,dc}}$ for the triangular currents i_{m1} and i_{m2} in steady state, cf. (7), directly yields the initial values of the currents:

$$I_{\mathrm{m1},0} = I_{\mathrm{m1,dc}} - \frac{d_1 V_{1,\mathrm{I}}}{2 f_\mathrm{s} L_{\mathrm{m1}}} \tag{19}$$

$$I_{\mathrm{m2},0} = I_{\mathrm{m2,dc}} - \frac{d_2 V_{2,\mathrm{I}}}{2 f_\mathrm{s} L_{\mathrm{m2}}} \begin{cases} 1 - \frac{2\delta}{d_2'}, & \text{Case A} \\ 1 - \frac{2\delta'}{d_2}, & \text{Case B} \end{cases} \tag{20}$$

$$I_{12,0} = \tfrac{k}{1/n-k} I_{\mathrm{m1},0} - \tfrac{k}{n-k} I_{\mathrm{m2},0} \tag{21}$$

The initial terminal currents follow directly:

$$I_{1,0} = I_{\mathrm{m1},0} + I_{12,0}, \quad I_{2,0} = -I_{\mathrm{m2},0} + I_{12,0} \tag{22}$$

With the DC components and the initial values of all considered steady-state currents fully defined, the time-domain waveforms and RMS current values can be derived based on the applied voltages. The resulting expressions are presented in the next section.

IV. Resulting Currents

Based on the previous analysis of the CI currents, the time-domain current waveforms are formulated in this section. Furthermore, analytical expressions for the RMS values of the terminal currents as well as the currents in the switches and the primary-side capacitor(s) (cf. Fig. 1 and Fig. 2) are presented.

A. Time-domain currents

The steady-state time-domain currents in the inductors of the Π circuit for the applied terminal voltages shown in Fig. 4 are derived using the previously stated initial currents. All currents are piecewise linear functions of time due to the piecewise constant terminal voltages:

$$i_{\mathrm{m1}} = I_{\mathrm{m1},0} + \tfrac{V_{1,\mathrm{I}}}{L_{\mathrm{m1}}} \begin{cases} t, & 0 \le \frac{t}{T_\mathrm{s}} < d_1 \\ \frac{t - T_\mathrm{s}}{1 - 1/d_1}, & d_1 \le \frac{t}{T_\mathrm{s}} \le 1 \end{cases} \tag{23}$$

$$i_{\mathrm{m2}} = I_{\mathrm{m2},0} + \begin{cases} \tilde{i}_{\mathrm{m2,A}}, & \text{Case A} \\ \tilde{i}_{\mathrm{m2,B}}, & \text{Case B} \end{cases} \tag{24}$$

$$\tilde{i}_{\mathrm{m2,A}} = -\tfrac{d_2 V_{2,\mathrm{I}}}{d_2' L_{\mathrm{m2}}} \begin{cases} t, & 0 \le \frac{t}{T_\mathrm{s}} < \delta \\ \frac{\delta T_\mathrm{s} - d_2' t}{d_2}, & \delta \le \frac{t}{T_\mathrm{s}} < d_2 + \delta \\ t - T_\mathrm{s}, & d_2 + \delta \le \frac{t}{T_\mathrm{s}} \le 1 \end{cases} \tag{25}$$

$$\tilde{i}_{\mathrm{m2,B}} = \tfrac{V_{2,\mathrm{I}}}{L_{\mathrm{m2}}} \begin{cases} t, & 0 \le \frac{t}{T_\mathrm{s}} < d_2 - \delta' \\ \frac{T_\mathrm{s} - t - \delta' T_\mathrm{s}/d_2}{d_2'/d_2}, & d_2 - \delta' \le \frac{t}{T_\mathrm{s}} < \delta \\ t - T_\mathrm{s}, & \delta \le \frac{t}{T_\mathrm{s}} \le 1 \end{cases} \tag{26}$$

Note that stating i_{m1} and i_{m2} is sufficient to define all currents because i_{12} can be calculated using i_{m1} and i_{m2} with (11).

The CI terminal currents $i_1 = i_{\mathrm{m1}} + i_{12}$ and $i_2 = -i_{\mathrm{m2}} + i_{12}$ can also be calculated using i_{m1} and i_{m2}:

$$i_1 = \left(1+\tfrac{L_{\mathrm{m1}}}{L_{12}}\right) i_{\mathrm{m1}} - \tfrac{L_{\mathrm{m2}}}{L_{12}} i_{\mathrm{m2}} = \tfrac{1/n}{1/n-k} i_{\mathrm{m1}} - \tfrac{k}{n-k} i_{\mathrm{m2}} \quad (27)$$

$$i_2 = \tfrac{L_{\mathrm{m1}}}{L_{12}} i_{\mathrm{m1}} - \left(1+\tfrac{L_{\mathrm{m2}}}{L_{12}}\right) i_{\mathrm{m2}} = \tfrac{k}{1/n-k} i_{\mathrm{m1}} - \tfrac{n}{n-k} i_{\mathrm{m2}} \quad (28)$$

These general expressions for the currents in the time domain can e.g. be used to evaluate the instantaneous currents at any point during the switching period and specifically also at the switching instants, which will be discussed next.

B. Switched currents (terminal currents at switching instants)

In various converter topologies, the terminal currents of the CI at the switching instants are relevant to calculate the switching losses since these currents must be switched by the transistors. Examples are the converter circuits in Fig. 1 or Fig. 2. With the considered voltages, cf. Fig. 4, there are two switching instants on the primary side ($T_{\mathrm{S1,I/II}}$) and two on the secondary side ($T_{\mathrm{S2,I/II}}$), which are given by:

$$T_{\mathrm{S1,I}} = 0\,\mathrm{s}, \quad T_{\mathrm{S1,II}} = d_1 T_{\mathrm{s}} \quad (29)$$

$$T_{\mathrm{S2,I}} = \delta T_{\mathrm{s}}, \quad T_{\mathrm{S2,II}} = \begin{cases} (d_2+\delta)\,T_{\mathrm{s}}, & \text{Case A} \\ (d_2-\delta')\,T_{\mathrm{s}}, & \text{Case B} \end{cases} \quad (30)$$

The resulting switched terminal currents are not explicitly stated here but can easily be calculated by evaluating (27) and (28) at the switching instants (29) and (30).

In addition to the instantaneous current values, also the RMS currents are of interest for a converter optimisation. They are discussed in the following.

C. RMS terminal currents

The RMS currents at the terminals of the coupled inductor are e.g. relevant for calculating copper losses. Based on the time-domain current waveforms (27) and (28), the expressions for calculating the RMS values of the two terminals currents are found to be:

$$I_j = \sqrt{\tfrac{1}{T_{\mathrm{s}}} \int_{0\,\mathrm{s}}^{T_{\mathrm{s}}} i_j^2 \mathrm{d}t} = \sqrt{I_{j,\mathrm{dc}}^2 + I_{j,\mathrm{ac}}^2}, \quad j \in \{1,2\} \quad (31)$$

$$= \sqrt{I_{j,\mathrm{dc}}^2 + \tfrac{(a_j-b_j)^2+4a_jb_jc}{12(1-k^2)^2 L_0^2 f_{\mathrm{s}}^2}}$$

The coefficients introduced in (31) are defined below:

$$a_1 = \tfrac{1}{n} d_1 V_{1,\mathrm{I}}, \;\; a_2 = n d_2 V_{2,\mathrm{I}}, \;\; b_1 = k d_2 V_{2,\mathrm{I}}, \;\; b_2 = k d_1 V_{1,\mathrm{I}} \quad (32)$$

$$c = \begin{cases} c_{\mathrm{A}}, & \text{Case A} \\ c_{\mathrm{B}}, & \text{Case B} \end{cases} \quad (33)$$

$$c_{\mathrm{A}} = \begin{cases} \frac{d_2' - (1+d_{12})^2 + 3\delta\left(d_{12}+\delta'\right)}{d_1' d_2'}, & 0 < d_1 < \delta \\ \frac{d_{12}^2 - 3\delta(d_{12}-\delta) - \frac{\delta^3}{d_1 d_2'}}{d_1' d_2}, & \delta \le d_1 < \delta + d_2 \\ \frac{d_{12}^2 - 3\delta(d_{12}-\delta)}{d_1 d_2'}, & d_2 + \delta \le d_1 < 1 \end{cases} \quad (34)$$

$$c_{\mathrm{B}} = \begin{cases} \frac{d_{12}^2 + 3\delta'\left(d_{12}+\delta'\right)}{d_1' d_2}, & 0 < d_1 < d_2 - \delta' \\ \frac{d_{12}^2 + 3\delta'\left(d_{12}+\delta'\right) - \frac{\delta'^3}{d_1' d_2}}{d_1 d_2'}, & d_2 - \delta' \le d_1 < \delta \\ \frac{d_2 - (1-d_{12})^2 - 3\delta'(d_{12}-\delta)}{d_1 d_2}, & \delta \le d_1 < 1 \end{cases} \quad (35)$$

Note that in (31) the RMS values of the AC components of the terminal currents are given as well. Next, the RMS values of the currents in the switches are derived.

D. Currents in the switches

To derive expressions for calculating the RMS currents in the switches shown in Fig. 1, or equivalently in Fig. 2, the DC components of the respective currents are derived first. They are given by the integrals in (36), (37) and (38), which are constrained to the two intervals (*I* or *II*, cf. Fig. 4):

$$I_{1,\mathrm{I,dc}} = \tfrac{\int_{\mathrm{I}} i_1 \mathrm{d}t}{T_{\mathrm{s}}} = d_1 \left(I_{1,\mathrm{dc}} + \tfrac{c_{\mathrm{dc}} d_2 V_{2,\mathrm{I}}}{2 d_2' L_{12} f_{\mathrm{s}}}\right) \quad (36)$$

$$I_{2,\mathrm{I,dc}} = \tfrac{\int_{\mathrm{I}} i_2 \mathrm{d}t}{T_{\mathrm{s}}} = d_2 \left(I_{2,\mathrm{dc}} + \tfrac{c_{\mathrm{dc}} d_1 V_{1,\mathrm{I}}}{2 d_1' L_{12} f_{\mathrm{s}}}\right) \quad (37)$$

$$I_{j,\mathrm{II,dc}} = \tfrac{\int_{\mathrm{II}} i_j \mathrm{d}t}{T_{\mathrm{s}}} = I_{j,\mathrm{dc}} - I_{j,\mathrm{I,dc}}, \quad j \in \{1,2\} \quad (38)$$

The newly introduced coefficient c_{dc} is defined below:

$$c_{\mathrm{dc}} = \begin{cases} c_{\mathrm{dc,A}}, & \text{Case A} \\ c_{\mathrm{dc,B}}, & \text{Case B} \end{cases} \quad (39)$$

$$c_{\mathrm{dc,A}} = \begin{cases} 1 + d_{12} - 2\delta, & 0 < d_1 < \delta \\ \left(2\delta - d_{12} - \frac{\delta^2}{d_1 d_2'}\right) \frac{d_2'}{d_2}, & \delta < d_1 < \delta + d_2 \\ \left(2\delta - d_{12}\right) \frac{d_1'}{d_1}, & \delta + d_2 < d_1 < 1 \end{cases} \quad (40)$$

$$c_{\mathrm{dc,B}} = \begin{cases} -\left(d_{12} + 2\delta'\right) \frac{d_2'}{d_2}, & 0 < d_1 < d_2 - \delta' \\ \left(\frac{\delta'^2}{d_1' d_2} - d_{12} - 2\delta'\right) \frac{d_1'}{d_1}, & d_2 - \delta' < d_1 < \delta \\ \left(1 + d_{12} - 2\delta\right) \frac{d_1' d_2'}{d_1 d_2}, & \delta < d_1 < 1 \end{cases} \quad (41)$$

The expressions for calculating the RMS values of the terminal currents are given by analogous integrals and can be written as functions of the DC components:

$$I_{j,\mathrm{I}} = \sqrt{\tfrac{1}{T_{\mathrm{s}}} \int_{0\,\mathrm{s}}^{T_{\mathrm{s}}} i_{j,\mathrm{I}}^2 \mathrm{d}t} = \sqrt{\tfrac{1}{T_{\mathrm{s}}} \int_{\mathrm{I}} i_j^2 \mathrm{d}t}, \quad j \in \{1,2\} \quad (42)$$

$$= \sqrt{d_j} \sqrt{\tfrac{I_{j,\mathrm{I,dc}}^2}{d_j^2} + \tfrac{(a_j + b_j \beta_{j,\mathrm{I}})^2 + 4 b_j^2 \gamma_{j,\mathrm{I}}}{12(1-k^2)^2 L_0^2 f_{\mathrm{s}}^2}}$$

$$I_{j,\mathrm{II}} = \sqrt{\tfrac{1}{T_{\mathrm{s}}} \int_{0\,\mathrm{s}}^{T_{\mathrm{s}}} i_{j,\mathrm{II}}^2 \mathrm{d}t} = \sqrt{\tfrac{1}{T_{\mathrm{s}}} \int_{\mathrm{II}} i_j^2 \mathrm{d}t}, \quad j \in \{1,2\} \quad (43)$$

$$= \sqrt{d_j'} \sqrt{\tfrac{I_{j,\mathrm{II,dc}}^2}{d_j'^2} + \tfrac{(a_j + b_j \beta_{j,\mathrm{II}})^2 + 4 b_j^2 \gamma_{j,\mathrm{II}}}{12(1-k^2)^2 L_0^2 f_{\mathrm{s}}^2}}$$

$$I_j^2 = I_{j,\mathrm{I}}^2 + I_{j,\mathrm{II}}^2, \quad j \in \{1,2\} \quad (44)$$

$$\beta_{j,\mathrm{I/II}} = \begin{cases} \beta_{j,\mathrm{A,I/II}}, & \text{Case A} \\ \beta_{j,\mathrm{B,I/II}}, & \text{Case B} \end{cases}, \quad \gamma_{j,\mathrm{I/II}} = \begin{cases} \gamma_{j,\mathrm{A,I/II}}, & \text{Case A} \\ \gamma_{j,\mathrm{B,I/II}}, & \text{Case B} \end{cases} \quad (45)$$

The newly introduced coefficients in (45) are given in Table I for case A and in Table II for case B. For the sake of brevity (and computational speed), not all coefficients are listed. Instead, the simplest expressions are selected s.t. all RMS values are nonetheless defined because (44) can be used together with (31), (42) and (43) to calculate the RMS values for which the coefficients are not explicitly listed.

E. Sum of terminal currents

The sum of the two CI terminal currents (denoted $i_{\mathrm{p}} = i_1 + i_2$) is of interest for some converter topologies. The CIBC in Fig. 1 is one example because the sum of the CI terminal

TABLE I
COEFFICIENTS FOR THE RMS CURRENTS IN THE SWITCHES (CASE A)

Coef.	$0 < d_1 < \delta$	$\delta \le d_1 < d_2{+}\delta$	$d_2{+}\delta \le d_1 < 1$
$\beta_{1,\mathrm{A,I}}$	$\frac{d_1}{d_2'}$	$\frac{(3d_1-2\delta)\delta^2}{d_1^2 d_2 d_2'} - \frac{d_1}{d_2}$	*Use $\beta_{1,\mathrm{A,II}}$ and (44).*
$\gamma_{1,\mathrm{A,I}}$	0	$\frac{(d_1-\delta)^3\delta^3}{d_1^4 d_2^2 d_2'^2}$	*Use $\gamma_{1,\mathrm{A,II}}$ and (44).*
$\beta_{1,\mathrm{A,II}}$	*Use $\beta_{1,\mathrm{A,I}}$ and (44).*	*Use $\beta_{1,\mathrm{A,I}}$ and (44).*	$-\frac{d_1'}{d_2'}$
$\gamma_{1,\mathrm{A,II}}$	*Use $\gamma_{1,\mathrm{A,I}}$ and (44).*	*Use $\gamma_{1,\mathrm{A,I}}$ and (44).*	0
$\beta_{2,\mathrm{A,I}}$	$\frac{d_2}{d_1'}$	*Use $\beta_{2,\mathrm{A,II}}$ and (44).*	$-\frac{d_2}{d_1}$
$\gamma_{2,\mathrm{A,I}}$	0	*Use $\gamma_{2,\mathrm{A,II}}$ and (44).*	0
$\beta_{2,\mathrm{A,II}}$	*Use $\beta_{2,\mathrm{A,I}}$ and (44).*	$\frac{(3d_2'-2\delta)\delta^2}{d_1 d_1' d_2'^2} - \frac{d_2'}{d_1'}$	*Use $\beta_{2,\mathrm{A,I}}$ and (44).*
$\gamma_{2,\mathrm{A,II}}$	*Use $\gamma_{2,\mathrm{A,I}}$ and (44).*	$\frac{(d_2'-\delta)^3\delta^3}{d_1^2 d_1'^2 d_2'^4}$	*Use $\gamma_{2,\mathrm{A,I}}$ and (44).*

TABLE II
COEFFICIENTS FOR THE RMS CURRENTS IN THE SWITCHES (CASE B)

Coef.	$0 < d_1 < d_2{-}\delta'$	$d_2{-}\delta' \le d_1 < \delta$	$\delta \le d_1 < 1$
$\beta_{1,\mathrm{B,I}}$	$-\frac{d_1}{d_2}$	*Use $\beta_{1,\mathrm{B,II}}$ and (44).*	*Use $\beta_{1,\mathrm{B,II}}$ and (44).*
$\gamma_{1,\mathrm{B,I}}$	0	*Use $\gamma_{1,\mathrm{B,II}}$ and (44).*	*Use $\gamma_{1,\mathrm{B,II}}$ and (44).*
$\beta_{1,\mathrm{B,II}}$	*Use $\beta_{1,\mathrm{B,I}}$ and (44).*	$\frac{d_1'}{d_2} - \frac{(d_1'+2\delta')(d_1'-\delta')^2}{d_1'^2 d_2 d_2'}$	$\frac{d_1'}{d_2}$
$\gamma_{1,\mathrm{B,II}}$	*Use $\gamma_{1,\mathrm{B,I}}$ and (44).*	$\frac{(d_1'-\delta')^3\delta'^3}{d_1'^4 d_2^2 d_2'^2}$	0
$\beta_{2,\mathrm{B,I}}$	*Use $\beta_{2,\mathrm{B,II}}$ and (44).*	$\frac{3d_2\delta'^2-2\delta'^3}{d_1 d_1' d_2^2} - \frac{d_2}{d_1}$	*Use $\beta_{2,\mathrm{B,II}}$ and (44).*
$\gamma_{2,\mathrm{B,I}}$	*Use $\gamma_{2,\mathrm{B,II}}$ and (44).*	$\frac{(d_2-\delta')^3\delta'^3}{d_1^2 d_1'^2 d_2^4}$	*Use $\gamma_{2,\mathrm{B,II}}$ and (44).*
$\beta_{2,\mathrm{B,II}}$	$-\frac{d_2'}{d_1'}$	*Use $\beta_{2,\mathrm{B,I}}$ and (44).*	$\frac{d_2'}{d_1}$
$\gamma_{2,\mathrm{B,II}}$	0	*Use $\gamma_{2,\mathrm{B,I}}$ and (44).*	0

currents represents the primary-side converter current. It can be generally written in terms of i_{m1} and i_{m2}:

$$\begin{aligned} i_{\mathrm{p}} &= I_{\mathrm{p,dc}} + i_{\mathrm{p,ac}} = i_1 + i_2 = i_{\mathrm{m1}} - i_{\mathrm{m2}} + 2i_{12} \\ &= \big(1{+}2\tfrac{L_{\mathrm{m1}}}{L_{12}}\big) i_{\mathrm{m1}} - \big(1{+}2\tfrac{L_{\mathrm{m2}}}{L_{12}}\big) i_{\mathrm{m2}} = \tfrac{1/n+k}{1/n-k} i_{\mathrm{m1}} - \tfrac{n+k}{n-k} i_{\mathrm{m2}} \end{aligned} \tag{46}$$

Its DC component $I_{\mathrm{p,dc}} = I_{1,\mathrm{dc}} + I_{2,\mathrm{dc}}$ is the sum of the two terminal DC components, which are assumed to be known. The AC component $i_{\mathrm{p,ac}} = i_{\mathrm{p}} - I_{\mathrm{p,dc}}$ is also of interest because a capacitor typically needs to buffer this component. The losses of such a capacitor can be modelled by a frequency-dependent equivalent series resistance (ESR). Therefore, the spectral composition of $i_{\mathrm{p,ac}}$ is generally of interest. However, a worst-case estimation of the capacitor losses can be obtained based on the capacitor's ESR at the switching frequency and the RMS value of the time-domain capacitor current. The expression for this RMS current can be written concisely by reusing the coefficient c, which was introduced in (33):

$$I_{\mathrm{p,ac}} = \sqrt{\tfrac{1}{T_{\mathrm{s}}} \int_{0\,\mathrm{s}}^{T_{\mathrm{s}}} i_{\mathrm{p,ac}}^2 \mathrm{d}t} = \sqrt{\tfrac{(a_{\mathrm{p}}-b_{\mathrm{p}})^2 + 4a_{\mathrm{p}}b_{\mathrm{p}}c}{12(1-k^2)^2 L_0^2 f_{\mathrm{s}}^2}} \tag{47}$$

$$a_{\mathrm{p}} = \big(\tfrac{1}{n}+k\big)\, d_1 V_{1,\mathrm{I}}, \quad b_{\mathrm{p}} = (n+k)\, d_2 V_{2,\mathrm{I}} \tag{48}$$

V. VALIDATION USING PLECS

Table III compares exemplary results of the presented analytical model with a lossless and a lossy PLECS simulation of the generalised circuit in Fig. 2 with parameters given in Fig. 4. The capacitors are thereby replaced by ideal voltage sources.

TABLE III
COMPARISON OF KEY RESULTS OF THE PRESENTED MODEL WITH PLECS USING THE CIRCUIT IN FIG. 2 AND PARAMETERS GIVEN IN FIG. 4

	Case	I_1	I_2	$I_{1,\mathrm{I}}$	$I_{2,\mathrm{I}}$	$I_{\mathrm{p,ac}}$
Presented model	A	28.128 A	31.957 A	14.148 A	22.175 A	42.876 A
PLECS (lossless)	A	28.128 A	31.957 A	14.148 A	22.175 A	42.876 A
PLECS (lossy)	A	28.101 A	31.801 A	14.083 A	22.227 A	42.646 A

The comparison confirms that the presented model is 100% accurate under lossless conditions. If winding resistances of $R_2 = R_1/n^2 = 50\,\mathrm{m\Omega}$ are considered and the duty cycles are adjusted to account for the associated losses, the model remains accurate to within a relative error of less than $\pm 1\%$.

VI. CONCLUSION

In this paper, an electric model of analytical expressions for the currents (time-domain, DC, RMS) in a general two-level converter topology with a two-winding CI is presented. The model assumes that periodic, rectangular (two-level) voltages with arbitrary phase shift, as well as steady-state duty cycles are applied to the windings of the CI.

The derived expressions are 100% accurate for the assumed conditions in the lossless case and enable a faster design process because relatively slow numerical simulations can be replaced with a fast analytical model.

Thanks to the generality of the introduced analytical model, it can not only be applied to the CIBC (Fig. 1) but also to a wide variety of other converters derived from the generalised topology in Fig. 2 with two-winding CIs or transformers.

REFERENCES

[1] M. Hirakawa, Y. Watanabe, M. Nagano, K. Andoh, S. Nakatomi, S. Hashino, and T. Shimizu, "High power DC/DC converter using extreme close-coupled inductors aimed for electric vehicles," *The 2010 International Power Electronics Conference*, pp. 2941–2948, 2010.

[2] G. Zhu, B. A. McDonald, and K. Wang, "Modeling and analysis of coupled inductors in power converters," *IEEE Transactions on Power Electronics*, vol. 26, no. 5, pp. 1355–1363, May 2011.

[3] X. Huang, F. C. Lee, Q. Li, and W. Du, "High-frequency high-efficiency GaN-based interleaved CRM bidirectional buck/boost converter with inverse coupled inductor," *IEEE Transactions on Power Electronics*, vol. 31, no. 6, pp. 4343–4352, Jun. 2016.

[4] R. Kitamoto, S. Sato, H. Nakamura, and A. Amano, "Development of fuel cell boost converter using coupled-inductor for new FCV," in *SAE Technical Paper Series*. SAE International, Mar. 2017.

[5] H. N. Tran, T.-T. LE, H. Jeong, S. Kim, and S. Choi, "A 300 kHz, 63 kW/L ZVT DC–DC converter for 800 V fuel cell electric vehicles," *IEEE Transactions on Power Electronics*, vol. 37, no. 3, Mar. 2022.

[6] M. Benzine, I. Salhi, A. Gaillard, and F. Gao, "Coupled inductors-based interleaved boost converters for fuel cell electric vehicles," in *2023 IEEE Transportation Electrification Conference & Expo (ITEC)*, Jun. 2023.

[7] F. Yang, X. Ruan, Y. Yang, and Z. Ye, "Interleaved critical current mode boost pfc converter with coupled inductor," *IEEE Transactions on Power Electronics*, vol. 26, no. 9, pp. 2404–2413, Sep. 2011.

[8] P.-L. Wong, P. Xu, P. Yang, and F. Lee, "Performance improvements of interleaving VRMs with coupling inductors," *IEEE Transactions on Power Electronics*, vol. 16, pp. 499–507, 2001.

[9] M. Pavlovsky, G. Guidi, and A. Kawamura, "Assessment of coupled and independent phase designs of interleaved multiphase buck/boost DC–DC converter for ev power train," *IEEE Transactions on Power Electronics*, vol. 29, no. 6, pp. 2693–2704, Jun. 2014.

[10] S. Kimura, Y. Itoh, W. Martinez, M. Yamamoto, and J. Imaoka, "Downsizing effects of integrated magnetic components in high power density dc–dc converters for ev and hev applications," *IEEE Transactions on Industry Applications*, vol. 52, no. 4, pp. 3294–3305, Jul. 2016.